



Adsorption profiles of rhodamine B and reactive orange 16 onto pharmaceutical-based activated charcoals

Muhamad Zulhalmie Mohd Nasir^{a,b}, Muhammad Abbas Ahmad Zaini^{a,b,*},
Mohd. Aziz Che Yunus^{a,b}

^aCentre of Lipids Engineering and Applied Research, Ibnu-Sina Institute for Scientific and Industrial Research, Universiti Teknologi Malaysia, 81310 UTM Johor Bahru, Johor, Malaysia, Tel. +607 5535552, email: abbas@cheme.utm.my (M.A.A. Zaini)

^bSchool of Chemical and Energy Engineering, Faculty of Engineering, Universiti Teknologi Malaysia, 81310 UTM Johor Bahru, Johor, Malaysia

Received 13 April 2018; Accepted 15 September 2018

ABSTRACT

The present study was aimed to characterize the adsorptive properties of pharmaceutical-based activated charcoals (Biocarbon and Dyna) for the adsorption of reactive orange 16 (RO16) and rhodamine B (Rh B). A commercial activated (CAC) was employed for comparison. The materials were characterized for textural properties and functional groups. Batch adsorption was evaluated at different concentrations of dyes and contact times. The adsorption data were analyzed using isotherm and kinetics models. Result shows that the specific surface area is in the order of CAC > Biocarbon > Dyna. The surface area of CAC is 909 m²/g, renders a higher removal of RO16 of 69.4 mg/g, while Biocarbon displays a higher removal of Rh B of 54.5 mg/g, despite a lower surface area of 172 m²/g. The adsorption data fitted well with Langmuir model and pseudo-kinetics models. The adsorption mechanisms of pharmaceutical-based activated charcoals are unique and may not necessarily dependent on surface area alone. The charcoals demonstrate a promising attribute as dyes adsorbent for wastewater treatment.

Keywords: Activated charcoal; Adsorption; Reactive orange 16; Rhodamine B

1. Introduction

Water pollution has been the menace in the world as water is essential for the survival of living organisms [1]. Hence, water pollution is a subject of considerable concern nowadays. Among the major source of water pollution is industrial effluent containing dyes. Dyes are essential substances used in the production of coloured textiles, and are also used in various industries such as food, paper, rubber, plastics, cosmetics and leather [2]. Dye consists of organic compound that can absorb visible wavelength due to the properties of its unsaturated structure. It is generally synthesized using chemicals of highly toxic and carcinogenic [3–6]. Dye effluent is usually in the

form of colored wastewater that is easily detected and traced back to its original sources [7]. The discharge of dye will inevitably damage the aquatic ecosystem. The presence of dye in the water body even at small concentration (≈ 1 mg/L) is highly visible, affecting the water transparency and oxygen solubility, and prevent light penetration, consequently depleting the respiration and photosynthesis processes [8–10]. Hence, the treatment of dye-containing wastewater is imperative, yet challenging due to its stability and resistant to physical, chemical and biological environment [11].

Several methods have been proposed to treat dyes wastewater [12,13]. Often, these methods have several drawbacks such as ineffective removal performance, expensive, high maintenance costs and less adaptable to

*Corresponding author.

dye-loaded wastewater. On the other hand, adsorption emerges as a promising, effective and convenient method to treat dye effluent due to its simple and straight forward process that is able to remove dyes at low concentration with high efficiency [14–18]. Adsorption is a process where the solid adsorbent captures the desired solute from water through diffusion into porous network by physical entrapment or chemical reaction. Generally, activated carbon has been widely used as adsorbent for adsorption due to its cavernous pore. However, the commercial activated carbon is produced from expensive precursor, and further it is difficult to regenerate the spent adsorbent for repetitive adsorption cycles. Thus, attention has now been shifted in searching for cheaper, sustainable and efficient alternatives such as agricultural by-products and activated charcoal.

Activated charcoal is normally used as oral medicine to cure overdoses and poisoning in conjunction with gastric emptying [19]. Activated charcoal is produced through pyrolysis of pulverized carbonaceous materials such as woods, coal and agricultural by-products at high temperature [20,21]. There are two methods to activate the charcoal, namely physical activation and chemical activation. For medical purpose, the preferable method is physical activation because it involves the use of inert, non-toxic oxidizing gases such as steam or CO₂ instead of using toxic chemical agents such as ZnCl₂ and KOH that are commonly used in chemical activation. Activated charcoal is also suitable to be used as adsorbent for wastewater treatment due to its unique surface chemistry and textural properties upon activation [22,23].

The use of pharmaceutical-based activated charcoals in wastewater treatment is not widely explored. This is due to the fact that the surface area of the adsorbent is small and the pore volume is not fully developed [21,24]. However, the promising adsorptive profiles of activated charcoals are still lack and not adequately explored and documented in much of published literature. Therefore, the present work aims at evaluating the dyes removal properties of two pharmaceutical-based activated charcoals, namely Dyna and Biocarbon. Commercial activated carbon was used for comparison. The adsorbent materials were characterized for BET surface area and surface functional groups. Rhodamine B (Rh B) and reactive orange 16 (RO16) were used as model pollutants. The adsorption data were analyzed using isotherm and kinetics models, and the mechanisms governing the adsorption were proposed.

2. Materials and methods

2.1. Materials

Two pharmaceutical-based activated charcoal, namely Dyna and Biocarbon were purchased from local pharmacy, and were ground to powder form for characterization and adsorption studies. Commercial activated carbon (CAC) was obtained from R&M Chemicals. Rhodamine B (abbr.: Rh B; molecular formula: C₂₈H₃₁ClN₂O₃; molecular weight: 479.02 g/mol) was purchased from R&M Chemicals. Rh B is a cationic and xanthinic dye (colour index number, C.I.: 45170) that is soluble in water (solubility, ~15 g/L), with maximum wavelength of 555 nm. The molecular structure

of Rh B is shown in Fig. 1a. Reactive Orange 16 (abbr.: RO16; molecular formula: C₂₀H₁₇N₃Na₂O₁₁S₃; molecular weight: 617.54 g/mol) was purchased from Sigma-Aldrich. RO16 is an anionic, single azo class dye (colour index, C.I.: 17757) with maximum wavelength of 494 nm. Fig. 1b shows the molecular structure of RO 16.

2.2. Characterization of adsorbents

The textural properties of activated charcoals and CAC were measured using a surface area analyzer (Micrometrics Pulse Chemisorb 2705). The surface functional groups were determined using a FTIR spectrometer (Perkin Elmer Spectrum One) over the frequency (wavenumber) range of 4000 cm⁻¹ to 400 cm⁻¹.

2.3. Adsorption studies

2.3.1. Adsorption equilibrium

The batch equilibrium experiments were carried out to evaluate the performance of adsorbents in removing Rh B and RO16 from aqueous solution. A dye stock solution was prepared by dissolving 1 g of dye powder in 1 L of distilled water. Dilution of stock solution to prepare batches of different initial concentrations: RO16 of 2 mg/L to 500 mg/L, and Rh B of 2 mg/L to 200 mg/L. For adsorption equilibrium, 0.03 g of adsorbent was added into a flask containing 30 mL of dye solution of specified concentration. The solution pH was not adjusted, and were measured as 6.19 ± 0.35 and 6.22 ± 0.50 for Rh B and RO16 solutions, respectively, for all initial concentrations studied. The flask was sealed, and the solid-solution mixture was allowed to equilibrate at room temperature for 72 h. The residual concentration was measured by UV-Vis spectrophotometer (Drawell) at

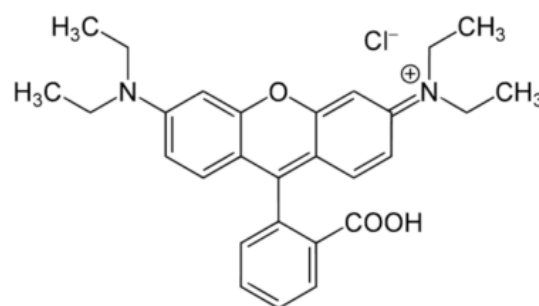


Fig. 1a. Chemical structure of rhodamine B.

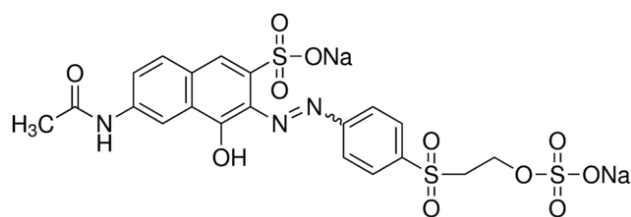


Fig. 1b. Chemical structure of reactive orange 16.

wavelengths of 494 nm and 555 nm for RO16 and Rh B, respectively. The adsorption capacity was calculated as $q_e = (C_o - C_e)V/m$, where q_e (mg/g) is the adsorption capacity at equilibrium, C_o (mg/L) and C_e (mg/L) are the initial and equilibrium concentrations, respectively, V (L) is the volume of dye solution and m (g) is the mass of the adsorbent.

2.3.2. Adsorption kinetics

A fixed adsorbent weight of 0.03 g was added into a flask containing 30 mL of dye solution of specified concentrations; 2 mg/L and 10 mg/L, and 5 mg/L and 20 mg/L for Rh B and RO16, respectively. These concentrations were selected based on the appreciable removal at equilibrium. The residual concentration was measured at different time intervals for 72 h, or until a constant removal was obtained. The adsorption capacity at time t , was computed as $q_t = (C_o - C_t)V/m$, where q_t (mg/g) is the adsorption capacity at time t , and C_t (mg/L) is the concentration measured at time t .

The equilibrium and kinetics data were analyzed using established models as summarized in Table 1, and were solved by non-linear regression except for Boyd and intraparticle diffusion models using linear regression [10,25].

3. Results and discussion

3.1. Characterization of adsorbents

The textural properties of pharmaceutical-based activated charcoals and commercial activated carbon (CAC) are shown in Table 2.

The specific surface area of CAC is superior compared to Dyna and Biocarbon, which is 909 m²/g. The specific surface area of Dyna and Biocarbon are lower probably due to insufficient or incomplete activation [21]. Table 2 also shows that Dyna and Biocarbon are highly mesoporous with average pore width of 5.27 and 2.54 nm, respectively, while CAC is rich in micropores with pore width centred at 1.94 nm. During the activation, the release of volatiles and restructuring of carbon backbone to form graphitic structure causing the increase in pore volume, hence increasing the specific surface area. CAC has a well-developed porous structure as a result of a complete activation [21].

The FTIR spectra of CAC, Dyna and Biocarbon are shown in Fig. 2. The broad and strong band at 3600–3100 cm⁻¹ is assigned to the stretching vibration of (–OH) hydroxyl group. For CAC, the band at 3600–3200 cm⁻¹ is normally assigned to moisture content, which is evident by two peaks at 4000–3600 cm⁻¹ [10,23–25]. The peak intensity decreased by the order of Dyna > Biocarbon > CAC. The peak at 3000–2850 cm⁻¹ shows the presence of alkyl group, –CH₂ vibration, where Dyna exhibits a higher intensity compared to Biocarbon. Alkene group is the attribute of a broad peak at 1680–1600 cm⁻¹ for activated charcoals and CAC, while C=C symmetric aromatic stretch at 1600–1500 cm⁻¹ exclusive for CAC signifies the development of graphitic structure. Peak at 1470–1350 cm⁻¹ indicates the CH₂ bending vibration, while the intense peak at 1200–900 cm⁻¹ is due to –CO stretching vibration. Generally, the FTIR spectra show that all adsorbents display almost similar functional groups.

3.2. Adsorption equilibrium

Fig. 3 shows the adsorption of reactive orange 16 (RO16) and rhodamine B (Rh B) onto activated charcoals and CAC at different initial concentrations. Dyna and CAC exhibit an increasing pattern of RO16 removal to a concentration of 400 mg/L. The removal capacity of CAC always higher than that of activated charcoals at all initial concentrations studied. Biocarbon displays an increase of RO16 removal to a maximum value at 50 mg/L. The maximum values of 72.2 mg/g, 51.1 mg/g and 25 mg/g were recorded at 400 mg/L for CAC, Dyna and Biocarbon, respectively. However, the peaks correspond to maximum removal percentage of 97.3%, 93% and 90.8% were attained at initial concentrations of 50 mg/L, 20 mg/L and 5 mg/L for CAC, Dyna and Biocarbon, respectively. The removal percentage decreases at higher concentration due to the decrease number of available sites as they have already been occupied by RO16 molecules, hence increasing the residual concentration upon adsorption. All three adsorbents also show an increasing removal of Rh B with increasing concentration. At initial concentration of 50 mg/L, Biocarbon gives the highest Rh B removal of 43.4 mg/g, followed by CAC (40 mg/g) and Dyna (25.5 mg/g). All adsorbents exhibit a high removal of Rh B of more than 95% at the concentrations studied, except Dyna that plummets from 93% to 53.5% at $C_o = 50$ mg/L.

In this work, the solution pH of RO16 and Rh B were not adjusted, and were measured as 6.19 ± 0.35 and 6.22 ± 0.50 , respectively. The molecular dimensions of RO16 and Rh B molecules are approximately 1.64 nm and 1.80 nm, respectively [28,29]. Fig. 4 shows the equilibrium curves of RO16 and Rh B. The removal of RO16 and Rh B were found to increase by the order of CAC>Dyna>Biocarbon, and Biocarbon>CAC>Dyna, respectively. The pattern of RO16 removal is somewhat in agreement with the role of surface area of adsorbents [28]. CAC with the highest surface area of 909 m²/g brings about the increase in interaction probabilities between the surface sites and RO16 molecules for high adsorption capacity. Despite a smaller surface area, interestingly the removal of RO16 by Dyna (2.07 m²/g) outweighs that of Biocarbon. This could be attributed to a high intensity of functional groups in Dyna as compared to that of Biocarbon. However, the removal pattern of Rh B is unique, that is neither completely surface area- nor surface groups-dependent. The average pore diameter could be the primary factor affecting the adsorption capacity. Biocarbon is more mesoporous than CAC, and has a bigger average pore diameter. Thus, the diffusion of Rh B dye molecules into Biocarbon channels is relatively easier [30]. On the other hand, Dyna with a greater pore width but limited access demonstrates a poorer removal of Rh B. The adsorption data were fitted using the commonly used isotherm models, and the isotherm constants are summarized in Table 3.

The maximum adsorption capacity, Q_m for RO16 removal onto Dyna, Biocarbon and CAC are 0.0745, 0.0356 and 0.112 mmol/g, respectively, while the corresponding values for Rh B adsorption are 0.0543, 0.114 and 0.0919 mmol/g, respectively. CAC displays a nearly equimolar removal of RO16 and Rh B, attributable to the restricted mesoporosity of activated carbon. Dyna shows a somewhat selective

Table 1
Isotherm and kinetics models

Isotherm models		
Langmuir	$q_e = \frac{Q_m b C_e}{(1 + b C_e)}$ $R_L = \frac{1}{1 + b C_o}$	q_e (mg/g) : Equilibrium adsorption capacity Q_m (mg/g) : Maximum adsorption capacity b (L/mg) : Langmuir isotherm constant C_e (mg/L) : Equilibrium concentration R_L : Separation factor C_o (mg/L) : Initial concentration
Freundlich	$q_e = K_F (C_e)^{1/n}$	K_F (mg/g)(L/mg) ^{1/n} : Freundlich isotherm constant n : Adsorption intensity
Redlich-Peterson	$q_e = \frac{K_R C_e}{(1 + a_R \cdot C_e^g)}$	K_R (L/g) : Redlich-Peterson isotherm constant a_R (L/mg) ^g : Redlich-Peterson isotherm constant g : Redlich-Peterson isotherm exponent
Temkin	$q_e = \frac{RT}{b_T} \ln A_T C_e$ $B = \frac{RT}{b_T}$	R (J/mol·K) : Universal gas constant T (K) : Absolute temperature A_T (L/mg) : Temkin isotherm equilibrium binding constant b_T (J/mol) : Temkin constant related to heat adsorption B : Temkin isotherm constant
Dubinin-Raduskevich	$q_e = Q_s \exp \exp \left(-K_{ad} \left(RT \ln \left(1 + \frac{1}{C_e} \right) \right)^2 \right)$ $E = \frac{1}{\sqrt{2K_{ad}}}$	Q_s (mg/g) : Theoretical isotherm saturation capacity K_{ad} (mol ² /kJ ²) : Dubinin-Raduskevich isotherm constant E (kJ/mol) : Mean free energy
Kinetics models		
Pseudo-first-order	$q_t = q_e [1 - \exp(-k_1 t)]$	q_t (mg/g) : Adsorption capacity at time, t k_1 (h ⁻¹) : Pseudo-first-order adsorption rate coefficient t (h) : Time
Pseudo-second-order	$q_t = \frac{k_2 q_e^2 t}{(1 + k_2 q_e t)}$ $h = k_2 q_e^2$	k_2 (g/mg·h) : Pseudo-second-order adsorption rate coefficient h (mg/g·h) : Initial adsorption rate
Intraparticle diffusion	$q_t = k_{diff} t^{0.5} + C$ $F = 1 - \frac{6}{\pi^2} \sum_{n=1}^{\infty} \frac{1}{n^2} \exp(-n^2 B t)$ $F = \frac{q_t}{q_e}$	k_{diff} (mg/g·h ^{0.5}) : Intraparticle diffusion coefficient C : Graph intersection F : Ratio of q_t to q_e B : Time constant
Boyd	For $F > 0.85$ $B t = -\ln \frac{\pi^2}{6} - \ln \ln(1 - F)$ For $F \leq 0.85$ $B t = \left(\sqrt{\pi} - \sqrt{\pi - \frac{\pi^2 F}{3}} \right)^2$	

Table 2
Textural properties of activated charcoals and CAC

	BET surface area (m ² /g)	Total pore volume (cm ³ /g)	Mesoporosity (%)	Average pore diameter (nm)
Dyna	2.07	0.003	100	5.27
Biocarbon	172	0.109	100	2.54
CAC	909	0.442	21.5	1.94

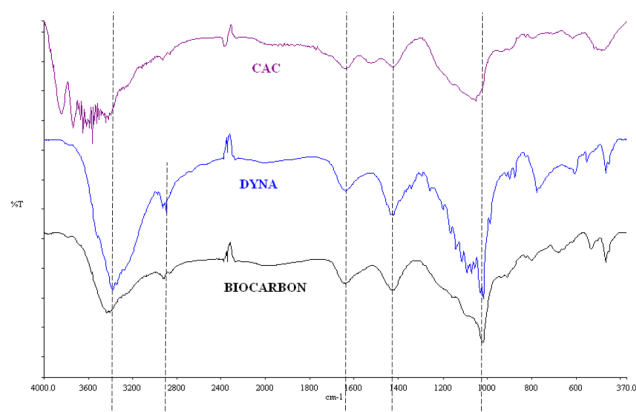


Fig. 2. FTIR analysis of pharmaceutical-based charcoals and CAC.

removal of RO16, while Biocarbon demonstrates a strong propensity of about 3.2 times towards Rh B. The unique adsorptive characteristics and selectivity signify the promising application of activated charcoals in dye-laden wastewater treatment.

The adsorption data were well-fitted into Langmuir model with R^2 closer to unity and small sum-of-squared error (SSE), implying the applicability of the model to describe the adsorption of RO16 and Rh B by activated charcoals and CAC. The separation factor, R_L suggests that the adsorption is favorable ($0 < R_L < 1$), and that the adsorption can be described as monolayer coverage of dyes molecules onto homogeneous surface of adsorbents.

The Freundlich constant, K_F is an indicator for adsorption capacity, while $1/n$ is a function to show the strength of adsorption. The $1/n$ values for both dyes are lesser than unity indicating that the adsorption is a standard Langmuir isotherm. Furthermore, the adsorption is favourable because the n values are between one to ten. The heterogeneity is expected to be greater for smaller $1/n$. Nevertheless, the Freundlich model fitting is not satisfactory to describe the adsorption data due to poor R^2 and SSE.

The Redlich-Peterson model combines the features of Langmuir and Freundlich models. From Table 3, the g values equal to 1 signifies that the model is purely a Langmuir-type. The Temkin model is used to describe the heat of adsorption on the surface that decreases linearly with the coverage and adsorbate-adsorbent interaction. The b_T of less than 20 kJ/mol indicates that the process is physisorption [31]. From the Dubinin-Raduschkevich model, the mean free energy, E of less than 8 kJ/mol indicates the physical adsorption [31]. The values of Q_s of Dubinin-Raduschkev-

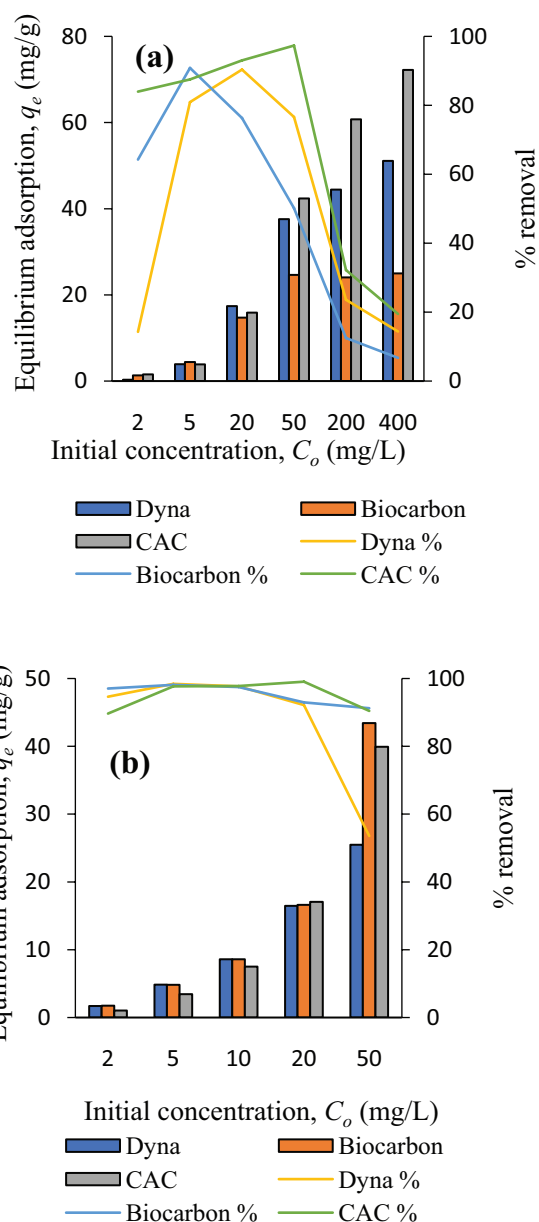


Fig. 3. Effect of initial concentration on adsorption of (a) RO16 and (b) Rh B onto activated charcoals and CAC.

ich model are in good agreement with Q_m of Langmuir model. The higher SSE values as displayed in Table 3 are due to the over-predicted q_e values as opposed to the experimental ones, especially at lower concentrations.

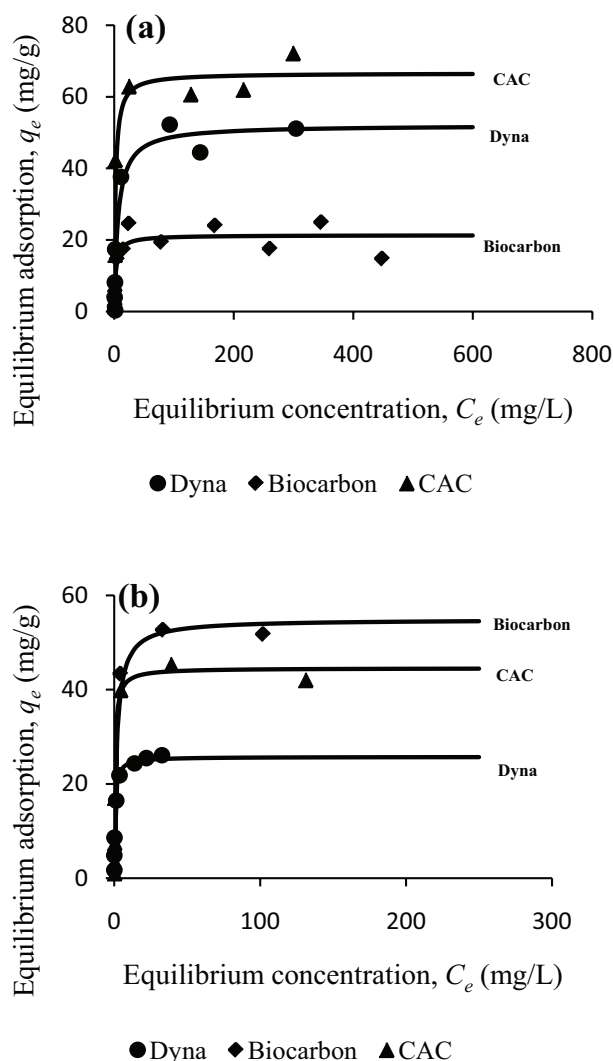


Fig. 4. Equilibrium adsorption of (a) RO16 and (b) Rh B by activated charcoals and CAC.

3.3. Adsorption kinetics

It is important to design the adsorption process to better understand the mechanisms and rate of adsorption. Fig. 5 shows the rate of adsorption of 5 and 20 mg/L of RO16, and 2 and 10 mg/L of Rh B by adsorbents. The rate of adsorption is normally high when dye molecules are initially in contact with adsorbent, until a period of time before it decreases.

Four kinetics models were used to analyze the rate of adsorption data, and the kinetics constants are summarized in Table 4. From Table 4, the rate of adsorption data are best fitted into the pseudo-first-order and pseudo-second order models.

The pseudo-first-order is based on the assumption that the rate of adsorption in bulk solution increases proportionally with the quantity of solute adsorbed, and that the process is physical adsorption [10]. The R^2 for pseudo-first-order model are satisfactorily to describe the RO16 and Rh B

Table 3a
Isotherm constants for RO16 removal by adsorbents

Isotherm models	Dyna	Biocarbon	CAC
$Q_{m,exp}$ (mg/g)	46	22	69.4
pH_e	6.59 ± 0.20	7.40 ± 0.03	7.29 ± 0.11
<i>Langmuir model</i>			
Q_m (mg/g)	52.1	21.3	66.6
b (L/mg)	0.151	0.364	0.442
R_L	0.016	0.005	0.006
R^2	0.936	0.812	0.904
SSE	468	38.5	91.2
<i>Freundlich model</i>			
K_F (mg/g)(L/mg) $^{1/n}$	11.8	9.44	20.0
n	3.60	6.85	4.35
$1/n$	0.278	0.146	0.230
R^2	0.812	0.545	0.788
SSE	613	81.7	164
<i>Redlich-Peterson model</i>			
K_R (L/mg)	7.85	7.76	29.4
a_R (L/mg) g	0.151	0.364	0.442
g	1.00	1.00	1.00
R^2	0.936	0.812	0.904
SSE	468	38.5	91.2
<i>Temkin model</i>			
A_T (L/mg)	2.04	19.1	7.14
b_T (J/mol)	0.285	0.963	0.261
B	8.69	2.57	9.48
R^2	0.895	0.639	0.862
SSE	477.898	58.447	87.152
<i>Dubinin-Raduskevich model</i>			
Q_S (mg/g)	47.097	20.431	64.561
K_{ad} (mol 2 /kJ 2)	1.302	1.037	0.346
E (kJ/mol)	0.620	0.694	1.20
R^2	0.923	0.833	0.930
SSE	419	29.6	31.8

adsorption onto activated charcoals and CAC. In addition, the pseudo-second-order model describes the chemical adsorption involving the exchange or sharing of electron between the solute and adsorbent via valency forces such as covalent forces and ion exchange [10]. The h indicates the initial rate of adsorption or affinity of adsorbent towards dye. Other factors such the characteristics of adsorbent and dye can also affect h . The rate of adsorption data are also fitted well into pseudo-second-order model with R^2 close to unity.

Fig. 6 shows the intraparticle diffusion model, with multi-linear lines. It indicates that there is more than one single kinetics stage during adsorption [25,32]. The first linear part of the graph can be attributed to intraparticle diffusion. It could be a slowest step in the adsorption, thus the rate limiting step. The second stage is diffusion through smaller pores, in which the equilibrium is later reached. For RO16 adsorption, all adsorbents display a two-stage except

Table 3b
Isotherm constants for Rh B removal by adsorbents

Isotherm models	Dyna	Biocarbon	CAC
$Q_{m,exp}$ (mg/g)	26	54.5	44
pH_e	6.37 ± 0.13	6.46 ± 0.28	7.60 ± 0.30
<i>Langmuir model</i>			
Q_m (mg/g)	25.8	54.9	44.6
b (L/mg)	1.68	0.552	1.63
R_L	0.008	0.009	0.003
R^2	0.979	0.976	0.951
SSE	23.8	19.8	104
<i>Freundlich model</i>			
K_f (mg/g)(L/mg) ^{1/n}	12.6	19.4	18.4
n	4.23	4.11	4.87
$1/n$	0.236	0.244	0.205
R^2	0.895	0.864	0.763
SSE	52.5	102	203
<i>Redlich-Peterson model</i>			
K_R (L/mg)	55.7	30.4	72.5
a_R (L/mg) ^g	2.53	0.552	1.627
g	0.946	1.00	1.00
R^2	0.983	0.976	0.951
SSE	25.0	19.8	105
<i>Temkin model</i>			
A_T (L/mg)	36.0	19.8	32.8
b_T (J/mol)	0.632	0.329	0.415
B	3.92	7.53	5.97
R^2	0.966	0.931	0.871
SSE	30.1	28.7	126
<i>Dubinin-Raduskevich model</i>			
Q_s (mg/g)	23.6	52.0	42.8
K_{ad} (mol ² /kJ ²)	0.056	0.552	0.062
E (kJ/mol)	2.99	0.952	2.83
R^2	0.934	0.989	0.957
SSE	25.06	43.8	86.0

for Biocarbon at concentration of 20 mg/L. For Rh B, Biocarbon and CAC exhibit a single stage at concentration of 2 mg/L, that is intraparticle diffusion.

The intraparticle diffusion model is used to interpret the kinetics data owing to the fact that the pseudo-kinetics models are inadequate to distinguish the effect of diffusion on adsorption. The assumption for intraparticle diffusion model is the only limiting step is intraparticle diffusion whereas the boundary layer or film diffusion is insignificant. From Table 4, the positive C suggests a rapid adsorption with controlling degree of film diffusion [10]. When C is negative, the boundary layer thickness retards the intraparticle diffusion as the mode of transport is influenced by two or more processes.

Fig. 7 shows the Boyd or film-diffusion model to elicit understanding on the mechanisms of RO16 and Rh

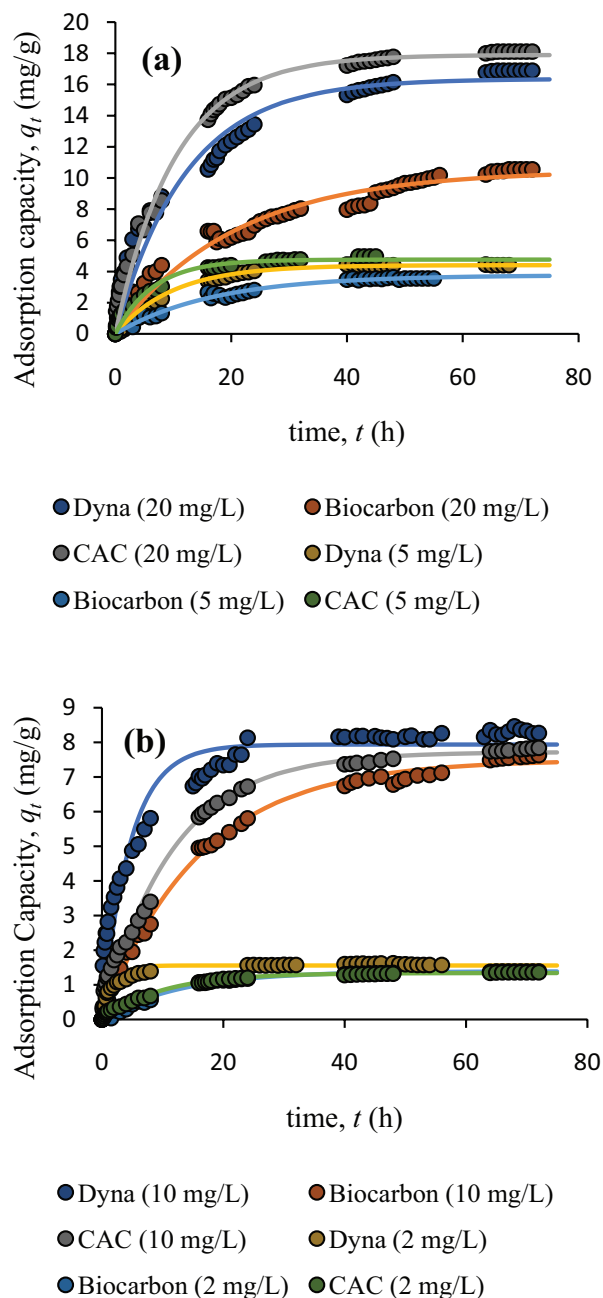


Fig. 5. Rate of adsorption of (a) RO16 and (b) Rh B.

B removal. The process of adsorption can be governed by either particle diffusion or film diffusion. From Table 4, the D_i values are in the range of 1.02×10^{-8} to 3.1×10^{-8} , indicating that the rate of control for this adsorption process is film diffusion which can be verified with the linearity of the graph which does not pass through origin [10,33].

4. Conclusion

The isotherm and kinetics of pharmaceutical-based activated charcoals and commercial active carbon (CAC) for

Table 4a
Kinetics constants for RO16 adsorption at 5 mg/L

Kinetics models	Dyna	Biocarbon	CAC
$q_{e,exp}$ (mg/g)	4.41	3.56	4.96
<i>Pseudo-first-order model</i>			
q_e (mg/g)	4.41	3.77	4.77
k_1 (h ⁻¹)	0.101	0.059	0.153
SSE (%)	9.73	5.56	14.9
R ²	0.990	0.986	0.985
<i>Pseudo-second-order model</i>			
q_e (mg/g)	5.14	4.92	5.56
k_2 (g/mg·h)	0.0239	0.0111	0.0334
h (mg/g·h)	0.631	0.268	1.03
SSE (%)	12.7	6.39	11.0
R ²	0.989	0.985	0.990
<i>Intraparticle diffusion model</i>			
k_{diff} (mg/g·h ^{0.5})	0.887	0.636	0.858
C (mg/g)	-0.207	-0.304	0.368
R ²	0.986	0.951	0.975
<i>Boyd model</i>			
B	0.081	0.070	0.090
D_i (cm ² /s)	1.47×10^{-8}	1.59×10^{-8}	2.52×10^{-8}
R ²	0.975	0.928	0.994

Table 4b
Kinetics constants for RO16 adsorption at 20 mg/L

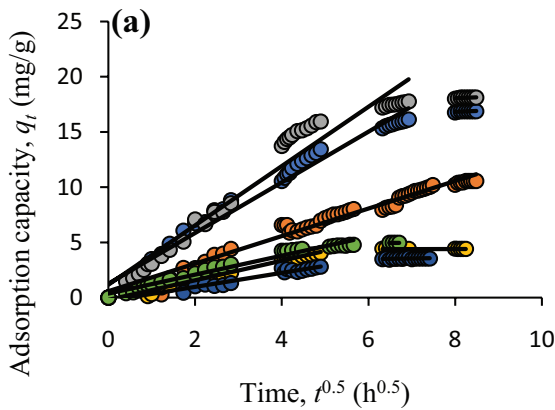
Kinetics models	Dyna	Biocarbon	CAC
$q_{e,exp}$ (mg/g)	16.9	10.6	18.1
<i>Pseudo-first-order model</i>			
q_e (mg/g)	16.4	10.5	17.9
k_1 (h ⁻¹)	0.0820	0.0486	0.0966
SSE (%)	17.3	11.1	12.0
R ²	0.976	0.964	0.994
<i>Pseudo-second-order model</i>			
q_e (mg/g)	18.8	13.2	20.6
k_2 (g/mg·h)	0.00593	0.00380	0.00595
h (mg/g·h)	2.09	0.664	2.53
SSE (%)	11.1	10.3	10.1
R ²	0.986	0.975	0.990
<i>Intraparticle diffusion model</i>			
k_{diff} (mg/g·h ^{0.5})	2.29	1.25	2.69
C (mg/g)	1.26	0.588	1.16
R ²	0.976	0.971	0.947
<i>Boyd model</i>			
B	0.0567	0.0499	0.0708
D_i (cm ² /s)	1.02×10^{-8}	1.14×10^{-8}	1.99×10^{-8}
R ²	0.957	0.845	0.994

Table 4c
Kinetics constants for Rh B adsorption at 2 mg/L

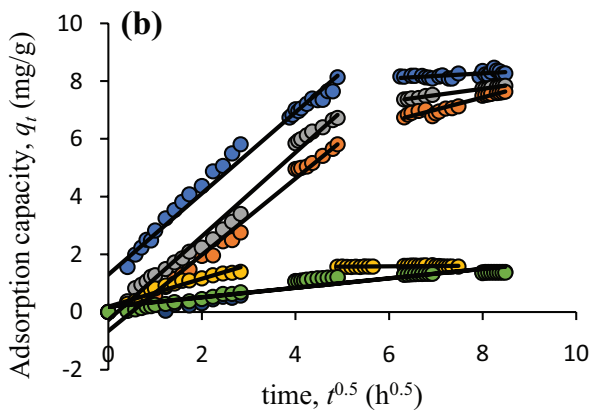
Kinetics models	Dyna	Biocarbon	CAC
$q_{e,exp}$ (mg/g)	1.58	1.39	1.36
<i>Pseudo-first-order model</i>			
q_e (mg/g)	1.56	1.39	1.34
k_1 (h ⁻¹)	0.532	0.079	0.100
SSE (%)	7.88	12.6	9.45
R ²	0.963	0.992	0.995
<i>Pseudo-second-order model</i>			
q_e (mg/g)	1.63	1.67	1.55
k_2 (g/mg·h)	0.508	0.052	0.082
h (mg/g·h)	1.351	0.145	0.196
SSE (%)	3.65	18.4	7.36
R ²	0.992	0.978	0.992
<i>Intraparticle diffusion model</i>			
k_{diff} (mg/g·h ^{0.5})	0.484	0.165	0.164
C (mg/g)	0.184	0.179	0.184
R ²	0.924	0.850	0.886
<i>Boyd model</i>			
B	0.169	0.068	0.068
D_i (cm ² /s)	3.1×10^{-8}	1.5×10^{-8}	1.9×10^{-8}
R ²	0.963	0.992	0.983

Table 4d
Kinetics constants for Rh B adsorption at 10 mg/L

Kinetics models	Dyna	Biocarbon	CAC
$q_{e,exp}$ (mg/g)	8.27	7.63	7.84
<i>Pseudo-first-order model</i>			
q_e (mg/g)	7.94	7.50	7.72
k_1 (h ⁻¹)	0.219	0.063	0.086
SSE (%)	12.2	8.00	14.6
R ²	0.954	0.997	0.993
<i>Pseudo-second-order model</i>			
q_e (mg/g)	8.57	9.31	9.07
k_2 (g/mg·h)	0.0392	0.0068	0.0111
h (mg/g·h)	2.88	0.591	0.914
SSE (%)	7.94	6.91	13.1
R ²	0.978	0.997	0.989
<i>Intraparticle diffusion model</i>			
k_{diff} (mg/g·h ^{0.5})	1.41	1.32	1.45
C (mg/g)	1.30	-0.657	-0.284
R ²	0.976	0.987	0.987
<i>Boyd model</i>			
B	0.073	0.051	0.063
D_i (cm ² /s)	1.32×10^{-8}	1.16×10^{-8}	1.77×10^{-8}
R ²	0.946	0.934	0.991



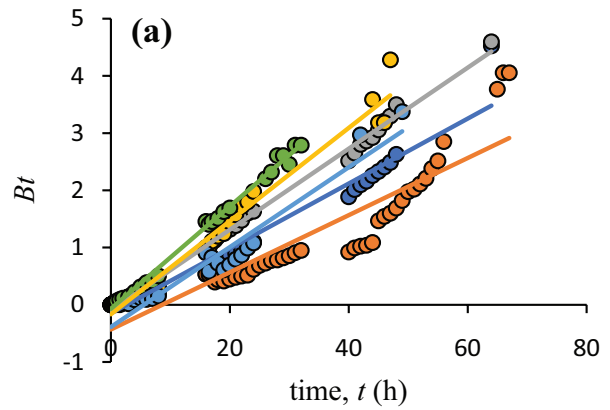
● Dyna (20 mg/L) ● Biocarbon (20 mg/L)
 ● CAC (20 mg/L) ● Dyna (5 mg/L)
 ● Biocarbon (5 mg/L) ● CAC (5 mg/L)



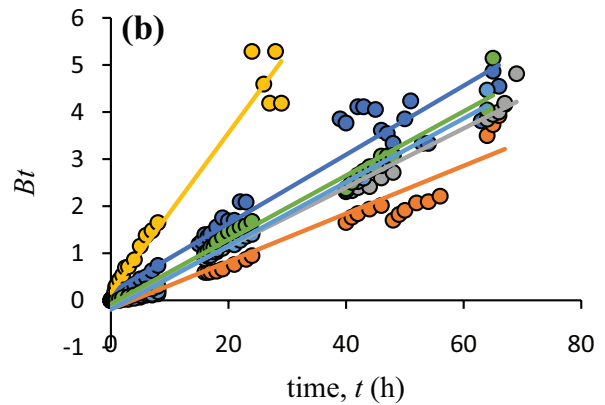
● Dyna (10 mg/L) ● Biocarbon (10 mg/L)
 ● CAC (10 mg/L) ● Dyna (2 mg/L)
 ● Biocarbon (2 mg/L) ● CAC (2 mg/L)

Fig. 6. Intraparticle diffusion for (a) RO16 and (b) Rh B removal onto activated charcoals and CAC.

reactive orange 16 (RO16) and rhodamine B (Rh B) removal were established. CAC (surface area = 909 m²/g, mesoporosity = 21.5%) exhibits a better performance for RO16, while Biocarbon (surface area = 172 m²/g, mesoporosity = 100%) demonstrates a higher removal of Rh B. Also, Biocarbon displays a selective removal of Rh B, that is 3.2 times greater than RO16. The pharmaceutical-based activated charcoals and CAC show a favourable adsorption towards dyes. The intraparticle diffusion could be the rate limiting step with some restriction of dyes diffusion due to film or boundary layer. This work reveals the feasibility of pharmaceutical-based activated charcoals as promising adsorbent with unique adsorption properties for dye-laden wastewater treatment.



● Dyna (20 mg/L) ● Biocarbon (20 mg/L)
 ● CAC (20 mg/L) ● Dyna (5 mg/L)
 ● Biocarbon (5 mg/L) ● CAC (5 mg/L)



● Dyna (10 mg/L) ● Biocarbon (10 mg/L)
 ● CAC (10 mg/L) ● Dyna (2 mg/L)
 ● Biocarbon (2 mg/L) ● CAC (2 mg/L)

Fig. 7. Boyd model for (a) RO16 and (b) Rh B removal onto activated charcoals and CAC.

Acknowledgment

The authors acknowledged the financial aid of UTM-Flagship grant No. 03G70.

References

[1] S. Shakoar, A. Nasar, Removal of methylene blue dye from artificially contaminated water using citrus limetta peel waste as a very low cost adsorbent, *J. Taiwan Inst. Chem. Eng.*, 66 (2016) 154–163.
 [2] S.W. Puasa, M.S. Ruzitah, A.S.A.K. Sharifah, Competitive removal of Reactive Black 5/Reactive Orange 16 from aqueous solution via micellar-enhanced ultra filtration, *Int. J. Chem. Eng. Appl.*, 3 (2012) 354–358.

- [3] Q.Z. Yong, M.A.A. Zaini, Adsorption of Rhodamine B by plum kernel shell adsorbents, *J. Eng. Technol.*, 7 (2016) 1–16.
- [4] L. Ma, R. Zhuo, H. Liu, D. Yu, M. Jiang, X. Zhang, Y. Yang, Efficient decolorization and detoxification of the sulfonated azo dye reactive orange 16 and simulated textile wastewater containing reactive orange 16 by the white-rot fungus *Ganoderma sp. En3* isolated from the forest of Tzu-chin Mountain in China, *Biochem. Eng. J.*, 82 (2014) 1–9.
- [5] M. Ghaedi, J. Tashkhourian, A.A. Pebdani, B. Sadeghian, F.N. Ana, Equilibrium, kinetic and thermodynamic study of removal of reactive orange 12 on platinum nanoparticle loaded on activated carbon as novel adsorbent, *Korean J. Chem. Eng.*, 28 (2011) 2255–2261.
- [6] D.Z. Mijin, V.D. Tomić, B.N. Grgur, Electrochemical decolorization of the reactive orange 16 dye using dimensionally stable Ti/PtOx anode, *J. Serbian Chem. Soc.*, 80 (2015) 903–915.
- [7] K. Kadirvelu, C. Karthika, N. Vennilamani, S. Pattabhi, Activated carbon from industrial solid waste as an adsorbent for the removal of Rhodamine-B from aqueous solution: Kinetic and equilibrium studies, *Chemosphere*, 60 (2005) 1009–1017.
- [8] D. Sun, Z. Zhang, M. Wang, Y. Wu, Adsorption of reactive dyes on activated carbon developed from *Enteromorpha prolifera*, *Am. J. Anal. Chem.*, 04 (2013) 17–26.
- [9] S. Syafalni, I. Abustan, I. Dahlan, C.K. Wah, G. Umar, Treatment of dye wastewater using granular activated carbon and zeolite filter, *Mod. Appl. Sci.*, 6 (2012) 37–51.
- [10] S.H. Tang, M.A.A. Zaini, Malachite green adsorption by potassium salts-activated carbons derived from textile sludge: Equilibrium, kinetics and thermodynamics studies, *Asia-Pacific J. Chem. Eng.*, 12 (2017) 159–172.
- [11] L. Li, S. Liu, T. Zhu, Application of activated carbon derived from scrap tires for adsorption of Rhodamine B, *J. Environ. Sci.*, 22 (2010) 1273–1280.
- [12] A. Sukhdev, A.S. Manjunatha, Puttaswamy, Decolorization of reactive orange 16 azo dye in wastewater using CAT/ IrCl₃/HClO₄ redox system: Delineation of kinetic modeling and mechanistic approaches, *J. Taiwan Inst. Chem. Eng.*, 70 (2017) 150–160.
- [13] T. Rasheed, M. Bilal, H.M.N. Iqbal, S.Z.H. Shah, H. Hu, X. Zhang, Y. Zhou, TiO₂/UV-assisted rhodamine B degradation: putative pathway and identification of intermediates by UPLC/MS, *Environ. Technol. (United Kingdom)*, 39 (2018) 1533–1543.
- [14] S. Nethaji, A. Sivasamy, A.B. Mandal, Adsorption isotherms, kinetics and mechanism for the adsorption of cationic and anionic dyes onto carbonaceous particles prepared from *Juglans regia* shell biomass, *Int. J. Environ. Sci. Technol.*, 10 (2013) 231–242.
- [15] K.Y. Foo, B.H. Hameed, Insights into the modeling of adsorption isotherm systems, *Chem. Eng. J.*, 156 (2010) 2–10.
- [16] G. Mezohegyi, A. Kolodkin, U.I. Castro, C. Bengoa, F. Stuber, J. Font, A. Fabregat, Effective anaerobic decolorization of azo dye acid orange 7 in continuous up flow packed-bed reactor using biological activated carbon system, *Ind. Eng. Chem. Res.*, 46 (2007) 6788–6792.
- [17] F. Marrakchi, M.J. Ahmed, W.A. Khanday, M. Asif, B.H. Hameed, Mesoporous carbonaceous material from fish scales as low-cost adsorbent for reactive orange 16 adsorption, *J. Taiwan Inst. Chem. Eng.*, 71 (2017) 47–54.
- [18] M. Bilal, M. Asgher, R. Parra-Saldivar, H. Hu, W. Wang, X. Zhang, H.M.N. Iqbal, Immobilized ligninolytic enzymes: An innovative and environmental responsive technology to tackle dye-based industrial pollutants – A review, *Sci. Total Environ.*, 576 (2017) 646–659.
- [19] R.W. Derlet, T.E. Albertson, Activated charcoal—past, present and future., *West. J. Med.*, 145 (1986) 493–496.
- [20] K.R. Olson, Activated charcoal for acute poisoning: one toxicologist's journey, *J. Med. Toxicol.*, 6 (2010) 190–198.
- [21] M.A.A. Zaini, N.A. Mohamad, Activated charcoal for oral medicinal purposes: Is it really activated?, *J. Appl. Pharm. Sci.*, 5 (2015) 157–159.
- [22] P. Gaudreault, Activated charcoal revisited, *Clin. Pediatr. Emerg. Med.*, 6 (2005) 76–80.
- [23] A.J. Alkhatib, K. Al Zailaey, Medical and environmental applications of activated charcoal, *Eur. Sci. J.*, 11 (2015) 50–57.
- [24] M.J. Iqbal, M.N. Ashiq, Adsorption of dyes from aqueous solutions on activated charcoal, *J. Hazard. Mater.*, 139 (2007) 57–66.
- [25] P. Senthil Kumar, C. Senthamarai, A. Durgadevi, Adsorption kinetics, mechanism, isotherm, and thermodynamic analysis of copper ions onto the surface modified agricultural waste, *Environ. Prog. Sustain. Energy*, 33 (2014) 28–37.
- [26] N. Alias, M.A.A. Zaini, M.J. Kamaruddin, Roles of impregnation ratio of K₂CO₃ and NaOH in chemical activation of palm kernel shell, *J. Appl. Sci. Process Eng.*, 4 (2017) 195–204.
- [27] M.A.A. Zaini, M.S.M. Shaid, Metal-chloride-activated empty fruit-bunch carbons for Rhodamine B removal, *Hungarian J. Ind. Chem.*, 44 (2016) 129–133.
- [28] T. Calvete, E.C. Lima, N.F. Cardoso, J.C.P. Vaghetti, S.L.P. Dias, F.A. Pavan, Application of carbon adsorbents prepared from Brazilian-pine fruit shell for the removal of reactive orange 16 from aqueous solution: Kinetic, equilibrium, and thermodynamic studies, *J. Environ. Manage.*, 91 (2010) 1695–1706.
- [29] Y. Guo, J. Zhao, H. Zhang, S. Yang, J. Qi, Z. Wang, H. Xu, Use of rice husk-based porous carbon for adsorption of Rhodamine B from aqueous solutions, *Dye. Pigment.*, 66 (2005) 123–128.
- [30] M.A.A. Zaini, L.W. Chai Li, M.J. Kamaruddin, S.H.M. Setapar, M.A. Che Yunus, Irradiated water-activated waste tyre powder for decolorization of reactive orange 16, *J. Teknol. (Sciences Eng)*, 68 (2014) 95–100.
- [31] A.U. Itodo, H.U. Itodo, Sorption energies estimation using Dubinin-Radushkevich and temkin adsorption isotherms, *Life Sci. J.*, 7 (2010) 31–39.
- [32] M. Sathishkumar, A.R. Binupriya, D. Kavitha, R. Selvakumar, K.K. Sheema, J.G. Choi, S.E. Yun, Organic micro-pollutant removal in liquid-phase using carbonized silk cotton hull, *J. Environ. Sci.*, 20 (2008) 1046–1054.
- [33] J.A. Alexander, M.A.A. Zaini, A. Surajudeen, E.N.U. Aliyu, A.U. Omeiza, Insight into kinetics and thermodynamics properties of multicomponent lead(II), cadmium(II) and manganese(II) adsorption onto Dijah-Monkin bentonite clay, *Part. Sci. Technol.*, (2018) 1–9.